Life Science Informatics Publications

Research Journal of Life Sciences, Bioinformatics, Pharmaceutical and Chemical Sciences

Journal Home page http://www.rjlbpcs.com/

RJLBPCS

ISSN 2454-6348

Original Research Article **DOI: 10.26479/2025.1202.02**

EXPLORING THE THERAPEUTIC POTENTIAL OF *ULVA LACTUCA* SULFATED POLYSACCHARIDES THROUGH *IN SILICO* DOCKING STUDIES

Neelima A[1], Lokanatha Valluru[1*], Kajal Chakraborty[2*],Shilpa Kamalakar Pai[2], Shubhajit Dhara[2]

1. Department of Biotechnology, Dravidian University, Kuppam-517426, Andhra Pradesh, India

2. Marine Bioprospecting Section of Marine Biotechnology, Fish Nutrition and Health Division, Central Marine Fisheries Research Institute, Ernakulam North P.O., P.B. No. 1603, Cochin-682018, Kerala, India.

ABSTRACT: Marine-derived sulfated polysaccharides have attracted increasing attention due to their diverse biological activities, particularly their immunomodulatory potential. In the present study, newly synthesized sulfated polysaccharides derived from *Ulva lactuca* were designed and evaluated for their immune-regulatory properties using structure-based molecular docking analysis performed with AutoDock 4. To elucidate their potential molecular mechanism, the polysaccharides were docked against key innate immune signaling proteins, including interleukin-10 (IL-10), nuclear factor kappa B (NF-κB), Toll-like receptor 4 (TLR-4), and tumor necrosis factor-alpha (TNF-α). For comparative analysis, standard immunomodulatory agents cyclophosphamide and levamisole were also subjected to docking studies with the same targets. The docking results revealed that sulfated polysaccharides exhibited higher binding affinity toward TLR-4 and TNF-α compared to the reference compounds. These proteins play crucial roles in activating the NF-κB signaling pathway within the innate immune system. The strong interactions observed suggest that the sulfated polysaccharides may enhance immune responses by modulating key inflammatory and immune signaling mediators. Overall, the findings indicate that sulfated polysaccharides derived from *Ulva lactuca* possess promising immunostimulatory potential and warrant further experimental validation to confirm their therapeutic applicability.

KEYWORDS: *Ulva lactuca*, AutoDock 4, Toll-like receptor 4 (TLR-4), Tumor necrosis factor-alpha (TNF-α), Nuclear factor kappa B (NF-κB), Interleukin-10 (IL-10).

Article History: Received: March 28, 2026; Revised: April 08, 2026; Accepted: April 10, 2026.

© 2026 Life Science Informatics Publication All rights reserved

Peer review under responsibility of Life Science Informatics Publications

Corresponding Author: Prof. Lokanatha Valluru Ph.D.

Department of Biotechnology, Dravidian University, Kuppam-517426, Andhra Pradesh, India

Email Address: lokanath.valluru@gmail.com

Graphical abstract

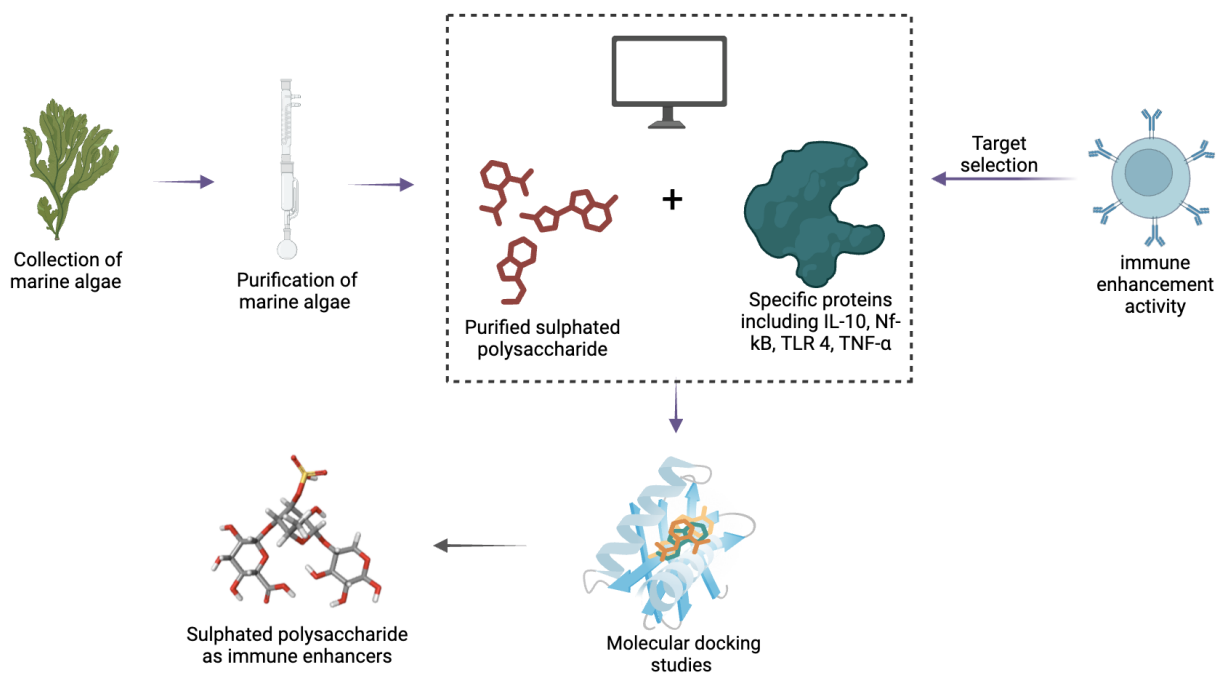

1. INTRODUCTION

Molecular docking describes the behavior of ligand at the binding site of target proteins and clarify basic biochemical processes by model the interaction between a ligand and a protein at the atomic level [1]. Predicting the ligand structure, together with its position and orientation within these sites (also referred to as pose), and evaluating the binding affinity are the two fundamental processes in the docking process. The efficiency of docking is greatly increased when the binding site's location is known prior to docking procedures [2]. A protein-ligand docking tool must include two fundamental components: sampling and scoring. Sampling is the process of generating probable ligand binding orientations/conformations around a protein binding site. It can be further separated into two aspects: ligand sampling and protein flexibility. Scoring is the prediction of binding

© 2026 Life Science Informatics Publication All rights reserved

tightness for specific ligand orientations/configurations using a physical or empirical energy function. The binding mode is projected to be the top orientation/conformation, which has the lowest energy score [3]. Fischer's [4] lock-and-key theory, in which the ligand fits into the receptor like a lock and key, provides an early explanation of the ligand-receptor binding mechanism. Based on this hypothesis, the first docking algorithms were described [5], treating the ligand and receptor as rigid entities. The lock-and-key hypothesis is then further developed by Koshland's "induced-fit" theory [6], which postulates that interactions between the ligands and the protein continuously remodel the protein's active region. According to this hypothesis, while docking, the ligand and receptor should be viewed as flexible. As a result, it might provide a more accurate description of the binding events than the rigid treatment. AutoDock 3.0 uses Monte Carlo simulated annealing, evolutionary, genetic, and Lamarckian genetic algorithms to represent ligand flexibility while maintaining the receptor stiff. The scoring function is based on the AMBER force field, which incorporates van der Waals, hydrogen bonding, electrostatic interactions, conformational entropy, and desolvation components. Each phrase is weighted based on an empirical scaling factor calculated from experimental data. AutoDock 4.0 can model receptor flexibility by enabling side chains to shift. In addition, this version of AutoDock allows for the evaluation of protein-protein docking interactions. The most recent version for molecular docking and virtual screening is AutoDock Vina [7]. The docking investigation was carried out with autodock 4, which is part of the MGL tools. The crystal structure of the IL-10, Nf-kB, MyD88, TLR-4, TNF-α protein was obtained from the Protein Data Bank. The PDB ID of the Il-10 (1VLK) , Nf-kB (1A3Q), TLR-4 (7MLM), TNF-α (2AZ5). Active site prediction for all proteins has been performed using discovery studio. The number of chains in IL-10 with one chain (A), Nf-kB with two chains (C & D), MyD88 with one chain (A), TLR- 4 with one chain (A), and TNF-α with four chains (A, B, C &D). Flexible docking was performed for all the five proteins.

2. MATERIALS AND METHODS

Sample collection and extraction of crude polysaccharide

Approximately 10 kg of seaweed sample was collected from Mandapam, Tamil Nadu, India (9.2724° N, 79.1287° E). Species identification was confirmed through comparison with reference specimens housed at the Marine Biodiversity Museum, Central Marine Fisheries Research Institute, India. The biomass was washed, shade-dried, and powdered. Pigments were removed through hexane extraction (37°C for 4–6 hours) followed by aqueous extraction 80–90°C for 5–8 hours at elevated temperatures. The extract was filtered using a 0.45 µm nylon cloth, concentrated, and subjected to ethanol precipitation (96%) at 4°C for 12 hours. The precipitate was collected, lyophilized, and yielded a sulfated polysaccharide with a recovery rate of 4.7% (w/w) relative to the initial dry weight.

© 2026 Life Science Informatics Publication All rights reserved

Isolation of polysaccharide and its purification

Synthesis of the crude polysaccharide (ULP) was carried out using an open glass column (25 cm × 4 cm) packed with DEAE cellulose as the stationary phase. The DEAE- cellulose (10 g) was prepared as a slurry in 50 mL of water and allowed to swell for three hours prior to column packing. After packing, the column was equilibrated with water. Approximately 2 g of the crude polysaccharide dissolved in 50 mL of water was loaded onto the DEAE-cellulose column. Elution was performed sequentially with double-distilled water, followed by stepwise gradients of sodium chloride (0–0.4 M NaCl). This procedure resulted in the separation.

Structures and Computational Tools

The structures used were: (a) the crystal structure of Il-10 (1VLK) , Nf-kB (1A3Q), TLR-4 (7MLM), TNF-α (2AZ5). (b) Sulphated polysaccharides from *ulva lactuca.* Computational tools used in this study included software tools: MGL Tools, AutoDock 4, Discovery Studio 2020 Client (DS), Open

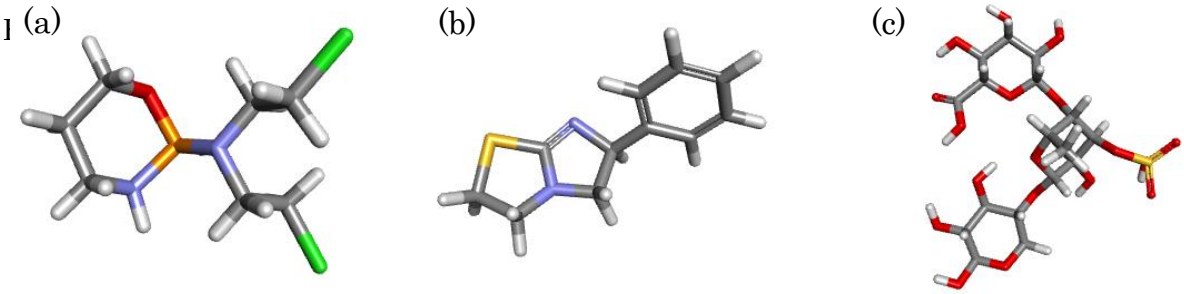

Figure 1: 3D images of (a) cyclophosphamide (b) levamisole and (c) sulfated polysaccharides

Receptor Preparation

The receptors (IL-10, Nf-kB, TLR-4, and TNF-α) included in this study were obtained from https://www.rcsb.org/. The corresponding receptors for IL-10, Nf-kB, TLR-4, and TNF-α were deposited [8,9,10, and 11]. AutoDockTools was used for preparation in order to add a hydrogen atom, remove water, ligand, and heteroatoms from the receptor, and determine its Gasteiger charge. After that, the file was saved as a PDBQT file and prepared for use with AutoDockTools in molecular docking. Using Discovery Studio, the receptors were also built in order to identify the covalent bonding, active site, and binding site based on the amino acid residue sequence.

© 2026 Life Science Informatics Publication All rights reserved

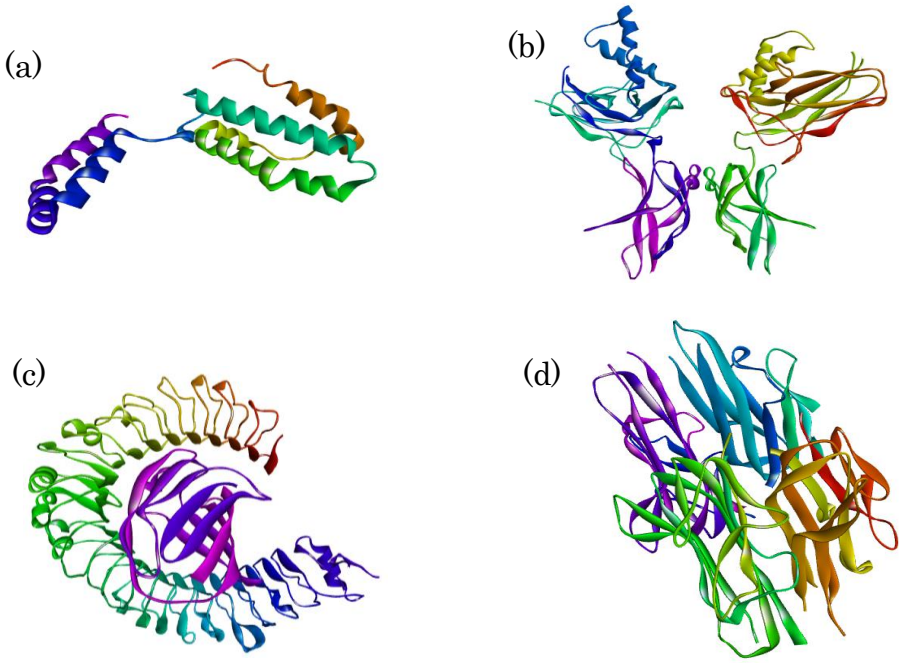

Figure 3.2: 3D images of (a) IL 10 (b) Nf-kb (c)TLR 4 (d)TNF-α

Ligand Preparation

ChemSketch was used to generate the ligand, which was then saved as a mol file. OpenBabel was then used to convert the mol files into PDB files [12]. After that, AutoDockTools transformed the PDB file into a PDBQT file, which was then prepared for use in the molecular docking simulation [13].

Molecular Docking Simulation

AutoDockTools and Discovery Studio were used to simulate molecular docking. Each of the four receptors' coordinates was established. Z = 38.50, Y = 6.94, and X = 81.51 had been established as the center of coordinates for IL-10. For TLR-4, the coordinate center was placed at X = 29.57, Y = 18.66, and Z = 24.17. The center of coordinates for Nf-kB was chosen at X = 10.00, Y = 82.32, and Z = 18.72. According to Table 1, the coordinate center for TNF-α was established at X = -35.13, Y = 65.88, and Z = 33.34. AutoDockTools was used to simulate ligands in the same locations. The docked structure data in PDBQT form and the binding affinity energy (ΔG) data were obtained from the molecular docking simulation.

© 2026 Life Science Informatics Publication All rights reserved

Table 1: Table showing the proteins and their grid parameter dimensions.

Sl.No	Name of the proteins	Center grid parameters
1	IL-10	81.51 x 6.94 x 38.50
2	Nf-kB	10.00 x 82.32 x 18.72
3	TLR 4	29.57 x 18.66 x 24.17
4	TNF-α	-35.13 x 65.88 x 33.34

Table 2: Table showing the Active site amino acids of all four proteins.

Sl.No	Name of the proteins	Active site amino acids
1	IL-10	Arg102, Arg104, Arg106, Arg107, Lys117, Lys119, Thr110, Gln113, and Ser114.
2	Nf-kB	Arg52, Arg54, His62, Val138, His140, Lys143, Lys221, Ser220, Ser222, Pro223, Asn227, Lys252, Lys283, and Tyr285.
3	TLR 4	Le32, Phe76, Leu78, Ile80, Asp99, Tyr102, Ser120, Phe121, Ile124, Phe126, Phe151, Leu293, Phe296, and Lys341.
4	TNF-α	Cys60, Lys89, Ser90, Pro91, Cys92, Gln93, Arg94, Thr96, Pro97, Lys103, Trp105, and Glu107.

3. RESULTS AND DISCUSSION

Molecular docking provides valuable insights into the interaction of ligand and biopolymers with immune regulatory proteins, thereby predicting their therapeutic potential. In this study, the ligands Cyclophosphamide, Levamisole, and sulfated polysaccharide were prepared and subjected to docking using AutoDock 4, with grid box dimensions optimized for the active site of the target proteins. The target proteins selected—IL-10, NF-κB, MyD88, TLR-4, and TNF-α are well-established modulators of immune responses, and their inhibition or modulation can influence both

© 2026 Life Science Informatics Publication All rights reserved

pro-inflammatory and anti-inflammatory signaling cascades.The ligands was prepared and saved as PDB structures to perform docking studies in autodock 4 to inhibit proteins. X, Y and Z co-ordinates for the grid are given in the table 1. In order to investigate the binding pattern and active site of Cyclophosphamide, Levamisole and sulfated polysaccharides with IL-10, Nf-kB, MyD88, TLR 4, TNF- α was accomplished by AutodockTools. Arg52, Arg54, His62, Val138, His140, Lys143, Lys221, Ser220, Ser222, Pro223, Asn227, Lys252, Lys283, and Tyr285 were among the amino acids found in the active site of Nf-kB. The primary binding groove contains Le32, Phe76, Leu78, Ile80, Asp99, Tyr102, Ser120, Phe121, Ile124, Phe126, Phe151, Leu293, Phe296, and Lys341 in the TLR-4's active site. The amino acids Arg102, Arg104, Arg106, Arg107, Lys117, Lys119, Thr110, Gln113, and Ser114 are the active site amino acids for IL-10. Cys60, Lys89, Ser90, Pro91, Cys92, Gln93, Arg94, Thr96, Pro97, Lys103, Trp105, and Glu107 are the amino acids that make up the active site of TNF-α (table 2).

The results indicates that Sulfated polysaccharide has higher affinity towards TNF-α with -12.02, TLR-4 with -11.09, IL-10 with -9.95 (table 3).

Interaction with IL-10

The sulphated polysaccharide exhibited significantly stronger binding of -9.95 against IL-10 (fig 3.3)with multiple hydrogen bonds and extra hydrophobic contacts. Levamisole (fig 3.2) and cyclophospham (A owe(B))hobic interactions and little hydro ɛx st

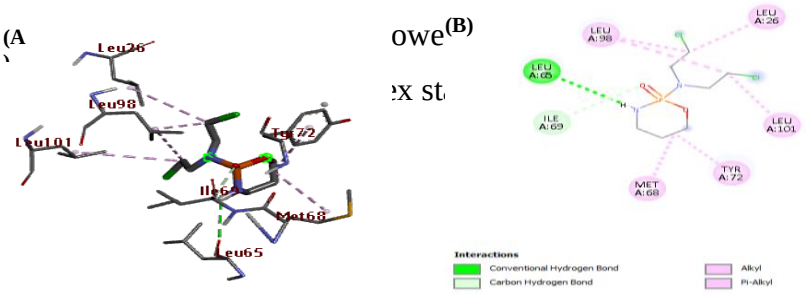

Figure 3.1: 3D image of IL-10 interaction with Cyclophosphamide. (b) 2D image of Cyclophosphamide with the active site amino acids.

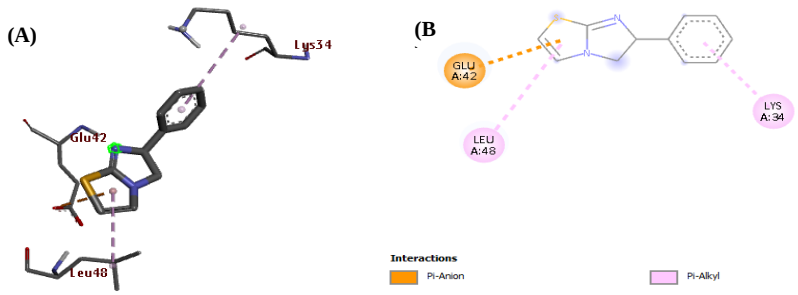

Figure 3.2: 3D image of IL-10 interaction with Levamisole. (b) 2D image of Levamisole with the active site amino acids.

© 2026 Life Science Informatics Publication All rights reserved

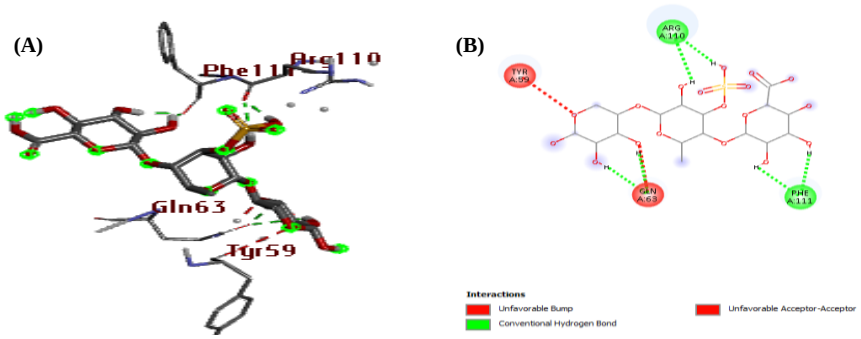

Figure 3.3: 3D image of IL-10 interaction with sulfated polysachharide. (b) 2D image of sulfated polysaccharide with the active site amino acids.

Interaction with Nf-kB

In the case of NF-κB, levamisole (fig 4.2) exhibited better binding than cyclophosphamide (fig 4.1), supported by hydrogen bonding and auxiliary non-covalent interactions with binding affinity of -7.35. Although the sulphated polysaccharide (fig 4.3) produced several hydrogen bonds with binding af

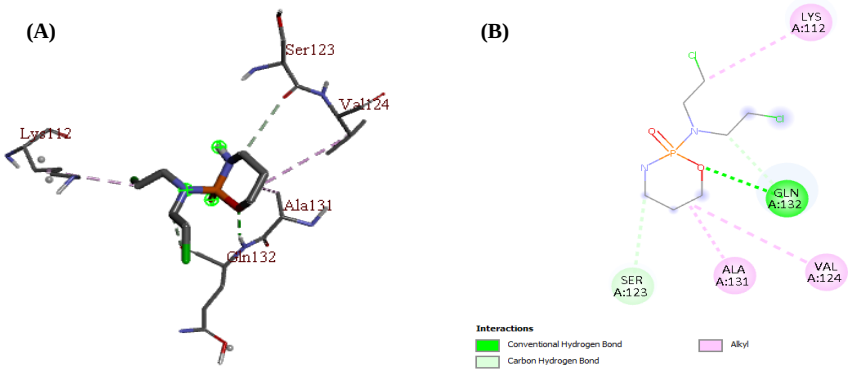

Figure 4.1: 3D image of Nf-kB interaction with Cyclophosphamide. (b) 2D image of cyclophosphamide with the active site amino acids.

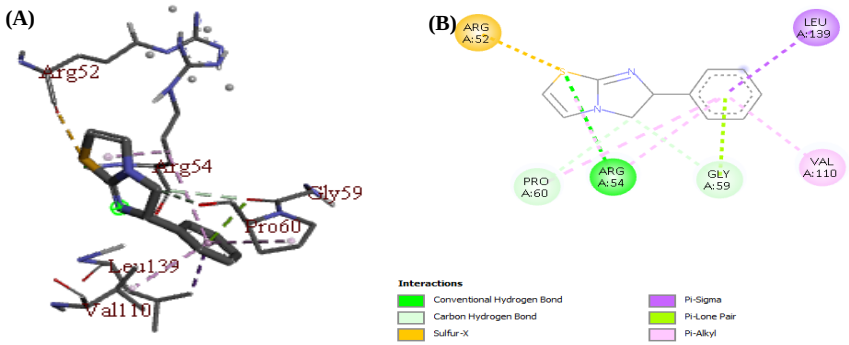

Figure 4.2: 3D image of Nf-kB interaction with levamisole. (b) 2D image of levamisole with the active site amino acids.

© 2026 Life Science Informatics Publication All rights reserved

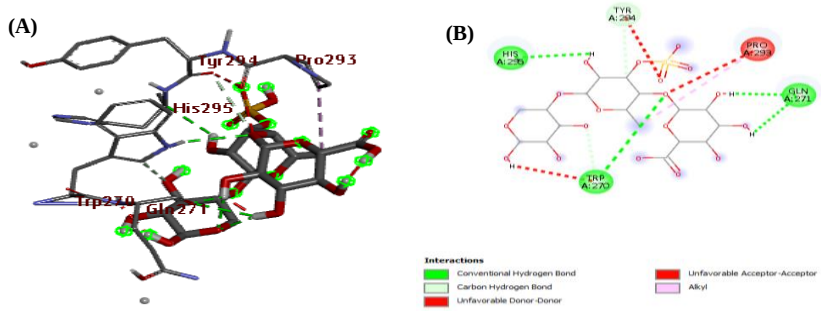

Figure 4.3: 3D image of Nf-kB interaction with sulfated polysaccharide. (b) 2D image of sulfated polysaccharide with the active site amino acids.

Interaction with TLR-4

The sulphated polysaccharide (fig 5.3) had the best binding profile of the three drugs, according to docking with TLR-4 (-11.09). It was distinguished by many hydrogen bonds and stable hydrophobic interactions inside the binding pocket. Levamisole (-6.82) and cyclophosphamide (-6.72) both exhibite zing connect

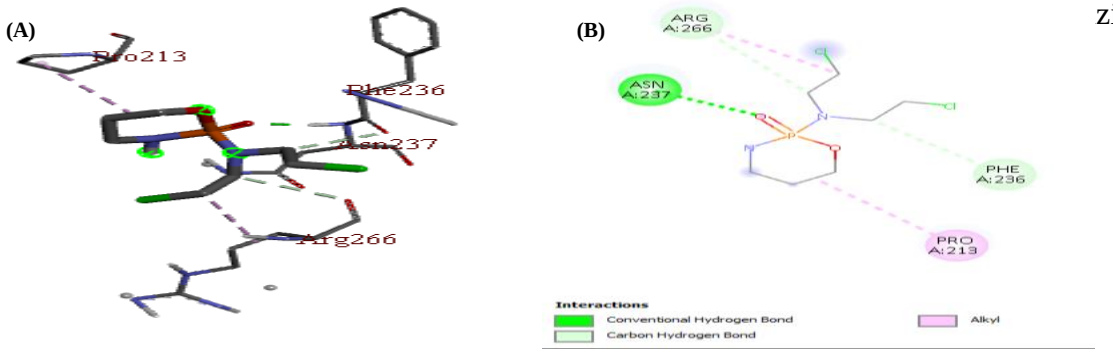

Figure 5.1: 3D image of TLR-4 interaction with Cyclophosphamide. (b) 2D image of Cyclophosphamide with the active site amino acids.

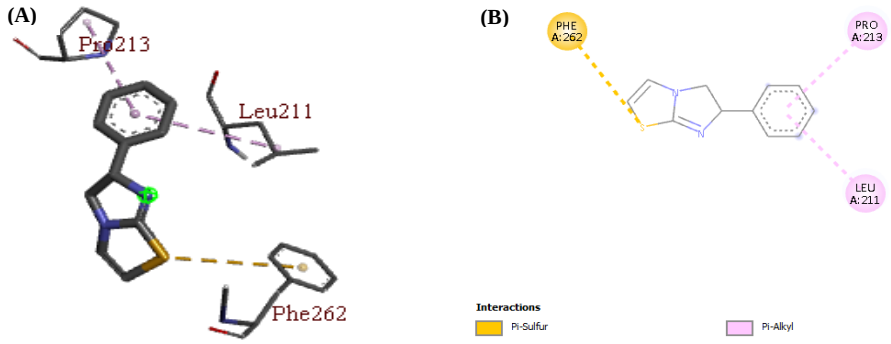

Figure 5.2: 3D image of TLR-4 interaction with Levamisole. (b) 2D image of levamisole with the active site amino acids.

© 2026 Life Science Informatics Publication All rights reserved

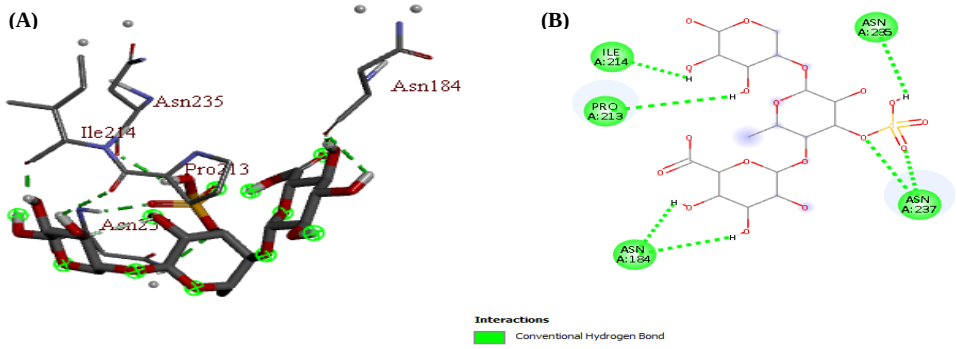

Figure 5.3: 3D image of TLR-4 interaction with sulfated polysaccharide. (b) 2D image of sulfated polysaccharide with the active site amino acids.

Interaction with TNF-α

The sulphated polysaccharide showed the strongest binding for TNF-α (-12.02), with complex stability being facilitated by many hydrogen bonds and hydrophobic interactions. Although both were noticeably weaker than the polysaccharide [illegible] higher affinity than cyc

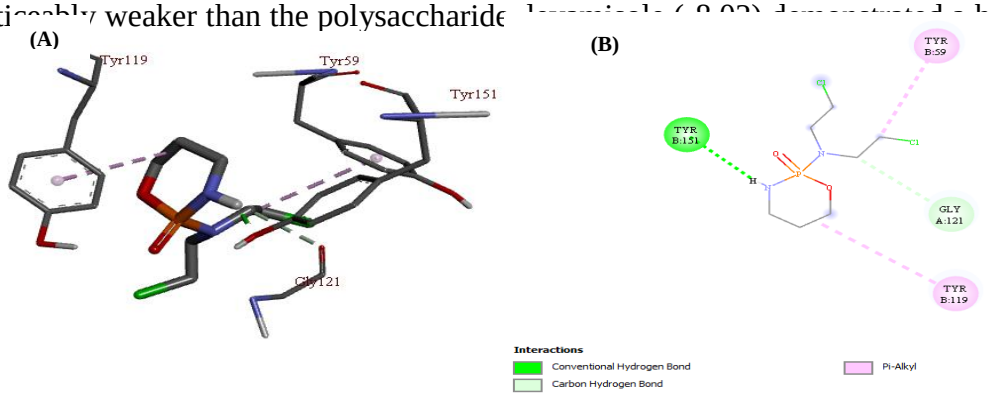

Figure 6.1: 3D image of TNF-α interaction with Cyclophosphamide. (b) 2D image of Cyclophosphamide with the active site amino acids

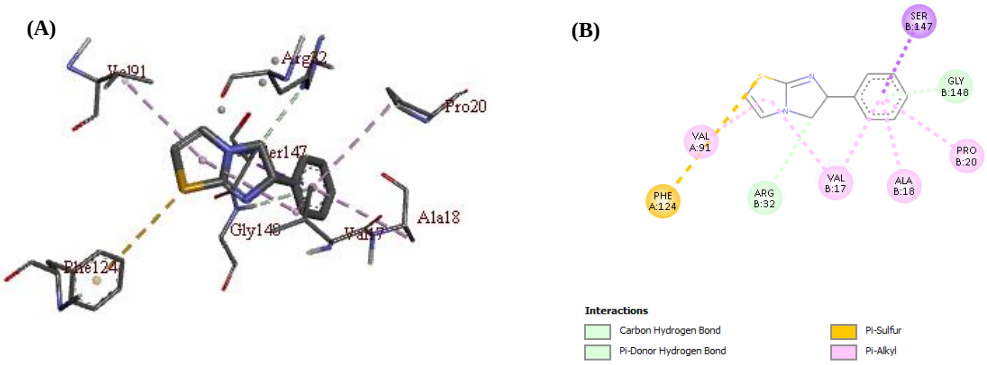

Figure 6.2: 3D image of TNF-α interaction with Levamisole. (b) 2D image of Levamisole with the active site amino acids.

© 2026 Life Science Informatics Publication All rights reserved

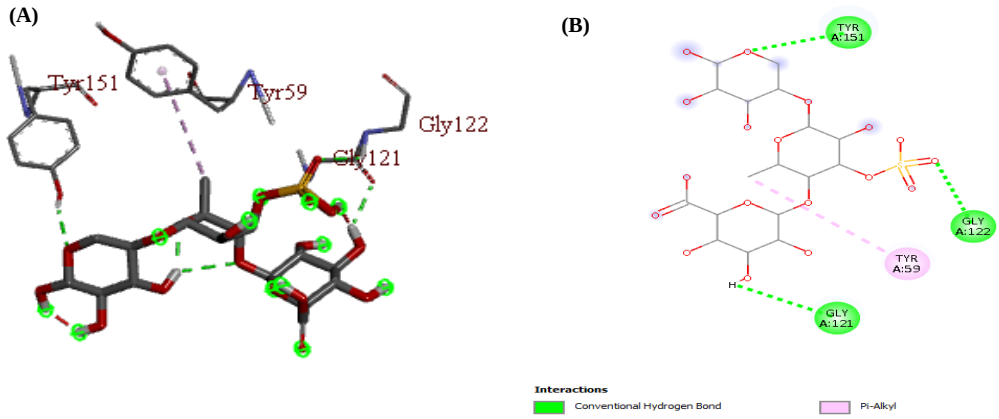

Figure 6.3: 3D image of TNF-α interaction with Sulfated polysaccharide. (b) 2D image of Sulfated polysaccharide with the active site amino acids.

These results suggested that the polysaccharide has a better interaction potential with immune surface receptors, thereby highlighting its possible role in modulating receptor-mediated signaling pathways. Molecular docking of sulfated polysaccharide with IL-10 revealed hydrogen bonds with Phe 111 and Arg 110 (Fig 3.3). The hydrogen and C-H bonds in between the sulfated polysaccharide and Nf-kB were Trp 270, Gln 271, His 295, and Tyr 294(Fig 4.3). Sulfated polysaccharide bound to TLR-4 formed five hydrogen bonds with Asn 184, Asn 237, Asn 235, Pro 213, and Ile 214 (Fig 5.3) . Sulfated polysaccharide interacts with TNF-α by forming three hydrogen bonds with Tyr 151, Gly 122, And Gly 121, and an alkyl bond was formed with Tyr 59 (Fig 6.3).

DISCUSSION

The docking results revealed that among the tested ligands, sulfated polysaccharide exhibited the strongest binding affinities, particularly with TNF-α (-12.02 kcal/mol), TLR-4 (-11.09 kcal/mol), and IL-10 (-9.95 kcal/mol). These binding energies indicate that the polysaccharide has a more stable and favorable interaction with immune surface receptors compared to Cyclophosphamide and Levamisole. Such high-affinity interactions suggest that sulfated polysaccharide may serve as an effective immunomodulatory candidate by targeting receptor-mediated pathways. Detailed interaction analysis demonstrated that the sulfated polysaccharide formed key hydrogen bonds with residues of immune receptors. With IL-10, interactions were observed with Phe111 and Arg110, indicating stabilization at the receptor's binding pocket (fig 3.3.3). In the case of NF-κB, hydrogen and C-H bonds were identified with Trp270, Gln271, His295, and Tyr294, residues critical for transcriptional regulation of inflammatory genes (fig 3.4.3). Similarly, the binding with TLR-4 involved five hydrogen bonds (Asn184, Asn237, Asn235, Pro213, and Ile214), highlighting a strong potential for receptor modulation (fig 3.5.3). Importantly, the docking with TNF-α revealed three

© 2026 Life Science Informatics Publication All rights reserved

hydrogen bonds (Tyr151, Gly122, Gly121) along with an alkyl interaction with Tyr59, further supporting the strong affinity of the polysaccharide (fig 3.6.3).

Table 3: Table showing the molecular docking results of all proteins.

Sl.No	Ligand	Protein	Rmsd	Binding energy	Inhibition constant	No of H bonds	Amino acids involved in interaction
1	Cyclophosphamide	IL-10	87.23	-5.69	66.93uM	1	H-bond: Leu 65 Pi Alkyl: Leu 98, Leu26, Leu 101, Tyr 72, Met 68. C-H bond: Ile 69
2	Levamisole		82.52	-6.35	22.32uM	-	Pi Alkyl: Leu 48, Lys 34
3	Sulphated Polysaccharide		80.59	-9.95	51.06nM	2	H-bond: Phe 111, Arg 110
4	Cyclophosphamide	Nf-kB	75.00	-5.97	41.82uM	1	H-bond: Gln 132 Alkyl: Lys 112, Val 124, Ala 131 C-H bond: Ser 123.
5	Levamisole		71.81	-7.35	4.08 uM	1	H-bond: Arg 54 C-H bond: Gly 59, Pro 60 Pi sigma: Ley 139 Pi Alkyl: Val 110
6	Sulphated		42.76	-6.22	27.37 uM	3	H-bond: Trp

© 2026 Life Science Informatics Publication All rights reserved

	Polysaccharide						270, Gln 271, His 295 C-H bond: Tyr 294
7	Cyclophosphamide	TLR-4	36.39	-6.72	11.86 uM	1	H-bond: Asn 237 C-H bond: Arg 266, Phe 236 Alkyl: Pro 213
8	Levamisole		36.25	-6.82	9.96 uM	-	Pi Alkyl: Pro 213 Leu 211 Pi sulfur: Phe 262
9	Sulphated Polysaccharide		37.44	-11.09	7.39 nM	5	H-bond: Asn 184, Asn 237, Asn 235, Pro 213, Ile 214
10	Cyclophosphamide	TNF-α	83.95	-7.63	2.56 uM	1	H-bond: Tyr 151 C-H bond: Tyr 59, Tyr 119 Pi Alkyl: Gly 121
11	Levamisole		90.60	-8.02	1.33 uM	-	C-H bond: Arg 32, Gly 148 Pi Alkyl: Val 91, Val 17, Ala 18, Pro 20 Pi sulfur: Phe 124 Pi sigma: Ser 147
12	Sulphated		82.05	-12.02	1.54 nM	3	H-bond: Tyr

© 2026 Life Science Informatics Publication All rights reserved

	Polysaccharide						151, Gly 122, Gly 121 Pi Alkyl: Tyr 59

Similar patterns have been documented for other bioactive substances isolated from Ginseng such as Rb2, which showed a strong affinity for IL-2 and stabilised the complex structure by creating three hydrogen bonds with Asp170, Val165, and Ala180 as well as a salt bridge with Lys45 [14]. Hydrogen bonds and electrostatic interactions played a important role in cytokine ligand recognition. The sulfated polysaccharide had greater interaction with TNF-α, TLR-4, and IL-10, whereas Rb2 associated preferentially with IL-2. This suggests that polysaccharide architectures of this type may have a variety of immunomodulatory effects by targeting distinct cytokines or receptor sites. The idea that sulfated polysaccharides, such as Rb2, can affect important immune regulatory proteins and thus function as promising natural immunomodulators is thus supported by the strong docking scores and interaction patterns. The immune-enhancing potential of these interactions can be explained through their biological relevance. TNF-α and NF-κB are central mediators of inflammatory responses, and modulation at these sites may help regulate excessive inflammation while supporting immune activation [15]. TLR-4, being a pattern recognition receptor, plays a critical role in innate immunity by activating downstream signaling cascades (e.g., MyD88–NF-κB) [16]. Strong binding of sulfated polysaccharide to TLR-4 suggests its possible role in triggering innate immune activation. Furthermore, IL-10, an anti-inflammatory cytokine, maintains immune homeostasis, and its binding with sulfated polysaccharide indicates a potential modulatory effect on balancing pro- and anti-inflammatory signals [17]. According to earlier reports on bioactive compounds from Albizia procera(AP), compounds like catechin, quercetin, isoquercetin, and other phytochemicals showed strong docking interactions with NF-κB p65, TNF-α, and IL-10 (binding energies ranging from -6.7 to -11.5 kcal/mol). These results are consistent with those findings. Interestingly, it was demonstrated that the AP phytochemicals formed hydrogen bonds with active site residues including Tyr119, Glu53, and Lys1 in TNF-α and Arg52, Lys221, and Tyr285 in NF-κB p52, indicating a potent inhibitory interaction with inflammatory proteins. However, they did not exhibit significant binding to IL-10, indicating a more selective inhibitory effect on pro-inflammatory mediators [18]. Similar results were found for another polysaccharide molecule, PSPP-1, which showed projected interaction energies of −5.6 kcal/mol for TLR-2 and −6.3 kcal/mol for TLR-4. This suggests that PSPP-1 may trigger receptor bioactivity and that it has a greater contact with TLR-4. Our sulfated polysaccharide's better affinity and improved binding stability with the receptor are further supported by its decreased binding energy (−11.09 kcal/mol with TLR-

© 2026 Life Science Informatics Publication All rights reserved

4) when compared to PSPP-1. Furthermore, a more persistent association is implied by the polysaccharide TLR-4 complex's larger number of hydrogen bonds, which could support receptor activation and subsequent immunological regulation [19]. However, limited binding affinity was observed toward IL-10, indicating a relatively selective inhibitory action against pro-inflammatory mediators. Similar molecular docking and mechanistic studies have shown that flavonoids such as quercetin and catechin can directly modulate NF-κB activation pathways and suppress TNF-α–mediated inflammatory responses [20, 21, 22]. Structural analyses further support that hydrogen bonding and electrostatic interactions with conserved residues within NF-κB and TNF-α are critical determinants of inhibitory potential [23, 24]. Collectively, these reports strengthen the evidence that AP-derived phytochemicals may exert anti-inflammatory effects through targeted modulation of NF-κB and TNF-α signaling pathways while sparing anti-inflammatory cytokines such as IL-10. Taken together, these results demonstrate that sulfated polysaccharide possesses significant binding affinity and interaction potential with key immune receptors, which may translate into enhanced immune responses by stabilizing receptor-ligand interactions and modulating cytokine signaling pathways. Thus, the docking results support the hypothesis that sulfated polysaccharides may act as natural immune-enhancing agents, potentially useful in combating immunosuppression and promoting host defense mechanisms.

4. CONCLUSION

In the conclusion, new sulfated polysaccharides from *Ulva lactuca* were created and put through a molecular docking analysis using Autodock 4. Sulfated polysaccharides, cyclophosphamide, and levamisole were docked with IL-10, Nf-kB, TLR-4, and TNF-α. Sulfated polysaccharides showed a higher binding affinity to TLR-4 and TNF-α, which are involved in the activation of the Nf-kB pathway in the innate immune system, suggesting that these polysaccharides may have immune-boosting qualities by activating immune proteins.

ETHICS APPROVAL AND CONSENT TO PARTICIPATE

Not applicable.

HUMAN AND ANIMAL RIGHTS

No animals or humans were used for the studies that are based on this research.

CONSENT FOR PUBLICATION

Not applicable.

FUNDING

None.

CONFLICT OF INTEREST

No

© 2026 Life Science Informatics Publication All rights reserved

ACKNOWLEGDEMENT

The authors gratefully acknowledge the financial support provided by Science & Engineering Research Board (SERB) of the DST, New Delhi, India. The authors are thankful to Dravidian University for providing facilities to carry out the work.

CONFLICT OF INTEREST

The authors declare that they have no known competing financial interests or personal relationships that could have appeared to influence the work reported in this paper.

REFERENCES

1. McConkey BJ, Sobolev V, Edelman M. The performance of current methods in ligand–protein docking. Curr Sci. 2002;845–856.
2. Meng XY, Zhang HX, Mezei M, Cui M. Molecular docking: a powerful approach for structure-based drug discovery. Curr Comput Aided Drug Des. 2011;7(2):146–157.
3. Huang SY, Zou X. Advances and challenges in protein-ligand docking. Int J Mol Sci. 2010;11(8):3016–3034.
4. Fischer E. Influence of configuration on the action of enzymes. Ber Dtsch Chem Ges. 1894;27(3):2985–2993.
5. Kuntz ID, Blaney JM, Oatley SJ, Langridge R, Ferrin TE. A geometric approach to macromolecule-ligand interactions. J Mol Biol. 1982;161(2):269–288.
6. Hammes GG. Multiple conformational changes in enzyme catalysis. Biochemistry. 2002;41(26):8221–8228.
7. Trott O, Olson AJ. AutoDock Vina: improving the speed and accuracy of docking with a new scoring function, efficient optimization, and multithreading. J Comput Chem. 2010;31(2):455–461.
8. Zdanov A, Schalk-Hihi C, Menon S, Moore KW, Wlodawer A. Crystal structure of Epstein-Barr virus protein BCRF1, a homolog of cellular interleukin-10. J Mol Biol. 1997;268(2):460–467.
9. Cramer P, Larson CJ, Verdine GL, Müller CW. Structure of the human NF-kappaB p52 homodimer-DNA complex at 2.1 A resolution. EMBO J. 1997;16(23):7078–7090.
10. Su L, Athamna M, Wang Y, Wang J, Freudenberg M, Yue T, et al. Sulfatides are endogenous ligands for the TLR4-MD-2 complex. Proc Natl Acad Sci U S A. 2021;118(30):e2105316118.
11. He MM, Smith AS, Oslob JD, Flanagan WM, Braisted AC, Whitty A, et al. Small-molecule inhibition of TNF-alpha. Science. 2005;310(5750):1022–1025.
12. O'Boyle NM, Banck M, James CA, Morley C, Vandermeersch T, Hutchison GR. Open Babel: an open chemical toolbox. J Cheminform. 2011;3:33.
13. Morris GM, Huey R, Lindstrom W, Sanner MF, Belew RK, Goodsell DS, et al. AutoDock4 and

© 2026 Life Science Informatics Publication All rights reserved

AutoDockTools4: automated docking with selective receptor flexibility. J Comput Chem. 2009;30(16):2785–2791.

14. Zheng S, Zheng H, Zhang R, Piao X, Hu J, Zhu Y, et al. Immunomodulatory effect of ginsenoside Rb2 against cyclophosphamide-induced immunosuppression in mice. Front Pharmacol. 2022;13:927087.
15. Liu T, Zhang L, Joo D, Sun SC. NF-κB signaling in inflammation. Signal Transduct Target Ther. 2017;2:17023.
16. Kawai T, Akira S. The role of pattern-recognition receptors in innate immunity: update on Toll-like receptors. Nat Immunol. 2010;11(5):373–384.
17. Saraiva M, O'Garra A. The regulation of IL-10 production by immune cells. Nat Rev Immunol. 2010;10(3):170–181.
18. Pasala PK, Netala S, Reddy Y, Sampath A, Neerugattu D, Mulukuri NVL, et al. Molecular docking and in vivo immunomodulatory activity of Albizia procera bark on doxorubicin-induced immunosuppressive rats. J King Saud Univ Sci. 2022;34:101828.
19. Ji C, Zhang Z, Chen J, Song D, Liu B, Li J, et al. Immune-enhancing effects of a novel glucan from purple sweet potato on RAW264.7 macrophage cells via TLR2- and TLR4-mediated pathways. J Agric Food Chem. 2021;69(38).
20. Liu Y, Shepherd EG, Nelin LD. MAPK phosphatases—regulating the immune response. Nat Rev Immunol. 2007;7(3):202–212.
21. Boots AW, Haenen GRMM, Bast A. Health effects of quercetin: from antioxidant to nutraceutical. Eur J Pharmacol. 2008;585(2–3):325–337.
22. Gupta SC, Tyagi AK, Deshmukh-Taskar P, Hinojosa M, Prasad S, Aggarwal BB. Downregulation of tumor necrosis factor and other pro-inflammatory biomarkers by polyphenols. Nutr Cancer. 2014;66(6):953–973.
23. Yadav VR, Prasad S, Sung B, Aggarwal BB. The role of chalcones in suppression of NF-κB–mediated inflammation. Biofactors. 2011;37(1):1–14.
24. Singh P, Arora A, Sharma S. Molecular docking studies of natural compounds as NF-κB inhibitors. Int J Mol Sci. 2016;17(6):817.

© 2026 Life Science Informatics Publication All rights reserved